Theoretical calculation of the Hall mobility of InN$_x$As$_{1-x}$ alloys when $x = 0.0$–0.1

SENEM AYDOGU[1,*], MUSTAFA AKARSU[2] and OMER OZBAS[2]

[1]Physics Department, Dumlupinar University, Kutahya, Turkey
[2]Physics Department, Eskisehir Osmangazi University, Eskisehir, Turkey
*Corresponding author. Email: saydogu@dumlupinar.edu.tr; aydou@yahoo.com

Abstract. The Hall mobility of InN$_x$As$_{1-x}$ semiconductor alloys is calculated by solving the Boltzmann transport equation using the iterative method. All the major scattering mechanisms are included in the calculations. The Hall mobilities of InAs and InN$_{0.01}$As$_{0.99}$ are presented in the temperature range of 30–600 K. It is shown that incorporation of even small amount of nitrogen leads to an abrupt reduction of the Hall mobility in InN$_x$As$_{1-x}$ at low temperatures. The effect of alloy random scattering on the Hall mobility of InN$_x$As$_{1-x}$ is examined at 77 and 300 K as the mole fraction x varies from 0.0 to 0.1. It is seen that the Hall mobility drops sharply up to $x = 0.02$ for 77 K and reduces slowly as the temperature increases to 300 K compared to 77 K. The Hall mobilities calculated theoretically are compared with the experimental data available in the literature.

Keywords. Semiconductor; Hall mobility; scattering mechanisms; InNAs.

PACS Nos 72.10.Di; 72.20.Dp; 72.20.Fr

1. Introduction

InAs is a narrow band-gap semiconductor belonging to III–V semiconductors and used in important technological applications. The high electron mobility of InAs, which is due to its narrow band gap, makes this compound useful for very high-speed and low-power electronic and infrared optoelectronic devices [1–3]. InN is as important as InAs because it is a key material for the manufacture of high-speed heterojunction transistors, ultraviolet (UV) detectors and UV light emitting diodes (LEDs) [4–7].

InN$_x$As$_{1-x}$ alloys obtained by the addition of InN and InAs compounds have recently attracted attention. The electronic properties of InN$_x$As$_{1-x}$ alloys are different from those of InAs and InN. Because the energy band gap of InN$_x$As$_{1-x}$ reduces significantly by adding a small amount of nitrogen to the InAs, the band gaps of InN$_x$As$_{1-x}$ alloys are expected to vary from 0.417 eV (InAs) to negative values, and then reach 0.7 eV (InN). These ternary alloys are used for manufacturing infrared detectors, gas sensors and the

lasers that operate in the whole infrared region [8–10]. Therefore, the works done on these ternary alloys deal with only specific concentrations of N and As [8,11–13].

The energy band gaps of InN_xAs_{1-x} alloys decrease rapidly leading to a strong disorder when a small amount of arsenic atoms in InAs is replaced by nitrogen. This occurs due to the large disparity in the electronegativity and the atomic size between N and As. The nitrogen atom induces several perturbations in the host crystal [15,16]. This is described as the band anticrossing (BAC) model [17–19]. The important characteristics of the model are: The energy band-gap reduction, the enhancement of the electron effective mass and the decrease of the electron mobility.

There are many experimental and theoretical studies on the band structure of InN_xAs_{1-x} and this alloy is a potential material for the optoelectronic devices operating in mid-infrared (2–8 μm) region at room temperature [8–22]. It is not enough to study the transport properties of InN_xAs_{1-x}. Hang *et al* examined the composition (x) dependence of mobility of InN_xAs_{1-x} besides increase in its effective mass by using the Shubnikov de Hass oscillations [10]. The physical and electrical properties of GaAsN and InAsN layers growth by liquid phase epitaxy technique was reported by Das *et al* [23]. The influence of the change of mobility on the composition (x) was experimentally investigated by Patane *et al* [24] and Zhuang *et al* [25]. The common point in these studies is the research done on the dependence of mobility on the composition (x). Kuboya *et al* reported the photoluminescence properties in relation to the carrier concentration of InAsN films grown by rf-plasma-assisted molecular beam epitaxy (RF-MBE) [26]. To investigate the effect of carrier concentration, the temperature dependence of Hall mobility was investigated using the van der Pauw methods in ref. [26]. We investigated the transport properties of InN_xAs_{1-x} to examine mostly the mobility as a function of composition (x). To perform this investigation, primarily the fraction range (x) of InN_xAs_{1-x} behaved as metallic was determined. Therefore, the composition x ($0.0 < x < 1.0$) dependence of the energy band gap in InN_xAs_{1-x} alloys was investigated. The Hall mobility of InN_xAs_{1-x} was calculated using an iterative method. The temperature dependence of the Hall mobility of InN_xAs_{1-x} ($x = 0.0, 0.01, 0.1218$), and the concentration (x) dependence of the Hall mobility of InN_xAs_{1-x} at 77 and 300 K were investigated.

2. Theoretical model

The Hall mobility is calculated by solving the Boltzmann transport equation using iterative method [27–29]. This equation involves various scattering mechanisms occurring in the material. In this work, the scattering mechanisms due to the acoustic phonon deformation potential, acoustic piezoelectricity, ionized impurities, alloy potential and polar optic phonons are taken into account.

The acoustic phonon deformation potential scattering rate is defined as [30]

$$S_{ac}(E) = \frac{\sqrt{2}E_1^2 k_B T_L m^{*3/2}}{\pi \rho \hbar^4 v_a^2} \gamma^{1/2} \frac{\gamma'}{2} \int_{-1}^{+1} (1-x) O(x) S_c(x) dx, \tag{1}$$

where E_1 is the acoustic deformation potential, T_L is the lattice temperature, m^* is the effective mass, ρ is the mass density, v_a is the sound velocity, γ is the band non-parabolicity, k_B is the Boltzmann constant, $\hbar$ is the Planck constant.

Acoustic phonon piezoelectric scattering rate can be defined as [30]

$$S_{pz}(E) = \frac{m^{*1/2}e^2 e_{14}^2 k_B T_L}{2\sqrt{2}\varepsilon_0^2 \pi \rho \hbar^2 v_a^2} \gamma^{-1/2} \frac{\gamma'}{2} \int_{-1}^{+1} O(x) S_c(x) dx, \tag{2}$$

where e is the electron charge, e_{14} is the piezoelectric constant, ε_0 is the permittivity.

The Brooks-Herring approach [31] is used for calculating the ionized impurity scattering rate. In this approach, the ionized impurity scattering rate is given by [30]

$$S_{im}(E) = \frac{N_I e^4}{16\sqrt{2}\pi \varepsilon_0^2 m^{*1/2}} \gamma^{-3/2} \gamma' \int_{-1}^{+1} \frac{1}{1-x} O(x) S_c(x) dx, \tag{3}$$

where N_I is the concentration of ionized impurity atoms.

The polar optic phonon scattering mechanism is produced as a result of the scattering of electrons with the potential that consists of the dipole moments that arise from the neighbour atoms changing place with opposite ionic charges [32]. The polar optic phonon scattering rate is expressed as [30]

$$S_{op}(E) = \frac{e^2 m^{*1/2}(\chi_s - \chi_\infty)k_B \theta_0}{4\sqrt{2}\pi \varepsilon_0 \hbar^2 \chi_s \chi_\infty [\exp(\frac{\theta_0}{T_L} - 1)]}$$
$$\times [F_+(E) + B_1 h(E - k_B \theta_0) F_-(E)], \tag{4}$$

where χ_∞ and χ_s are respectively high-frequency and low-frequency dielectric constants, θ_0 is the phonon Debye temperature. The other terms in eqs (1)–(4) can be found in ref. [30].

If binary compounds are used to produce the ternary alloys, they can be supposed to be dispersed at random, and their potentials are also dispersed randomly [33]. The alloy scattering takes place as a result of the scattering of the electrons due to this randomly distributed potential. The alloy scattering rate is taken as [28]

$$S_{al}(\vec{k}) = \frac{v_a x(1-x)(V_A - V_B)^2 m^*}{2\pi \hbar^3} \gamma'(E) k \int_{-1}^{+1} G(y) dy, \tag{5}$$

where v_a is the volume of the unit cell, x is the mole fraction, $V_A - V_B$ is the binary component potential. The other terms in eq. (5) can be found in ref. [33].

The structures of InAs, InN compounds and InN$_x$As$_{1-x}$ alloys are taken as cubic structures. It is supposed that these semiconductor compounds have direct band structures. Furthermore, the electron screening and mixing of s and p wave functions are taken into account.

In this work, it is accepted that InAs is doped with a small amount of nitrogen in the alloy formation process and the N atoms are randomly distributed in the InAs compound. For InN$_x$As$_{1-x}$ alloy ($0 < x \leq 0.1$), the cluster of As is more than the cluster of N, namely the presence of N atoms can be considered. This leads to the low lattice strain. Although Vegard's law is not valid due to the large size mismatch between InAs and InN [34], the validity of Vegard's law is accepted because of above approval in this study. Furthermore, in most studies [11,20,21,34], it is pointed out that the lattice constants of InN$_x$As$_{1-x}$ alloys depend on the concentration x and the impurity configuration when the N atoms are randomly distributed and so the validity of Vegard's law can be accepted.

Senem Aydogu, Mustafa Akarsu and Omer Ozbas

Table 1. The material parameters of the compounds used in the calculations.

Parameters	InAs	InN	Refs
High-frequency dielect. const.	11.74	6.7	[35,36]
Low-frequency dielect. const.	14.34	15.3	[35,37]
Polar phonon temperature (K)	337	846.3768	[35,38]
Mass density (kg/m^3)	5.667×10^3	6.81×10^3	[27,38]
Sound veloc. (m/s)	3.09×10^3	6.24×10^3	[27,39]
Piezoelec. const. (C/m^3)	0.0168	0.5	[40,41]
Acoustic deform. potential (eV)	5.8	7.1	[35,42]
Effective mass (m^*/m_0)	0.026	0.07	[13,38]
Lattice constant (Å)	6.058	4.98	[43,44]

The material parameters of InAs and InN compounds used in the calculations are given in table 1.

BAC model is reflected by the nonlinearity of the band-gap variation defined by the optical band gap bowing (a disorder parameter). The general representation of the composition-dependent band gap of the alloys involved in the deviation of the fundamental energy gap from linearity is

$$E_g(x) = xE_{InN} + (1-x)E_{InAs} - bx(1-x), \tag{6}$$

where b is the bowing parameter which is taken as 4.22 eV [12].

3. Results

The energy band gaps of the InN_xAs_{1-x} alloys are expected to vary from 0.417 eV to negative values, and then reach 0.7 eV by increasing x. First, the dependence of the energy band gap of InN_xAs_{1-x} alloys on concentration is investigated. Figure 1 shows the variation of band-gap as a function of the concentration x for the InN_xAs_{1-x} alloys. As shown in figure 1, the energy band-gap values of the InN_xAs_{1-x} alloys have negative values when the concentration x is in the range of 0.1218–0.8111. It reaches its minimum value of -0.5 eV at $x = 0.51$. These values are in agreement with the values in ref. [8]. The inset in figure 1 shows the detailed band-gap energy of InN_xAs_{1-x} alloy in the composition range of 0.0 to 0.1218. It can be seen that the band-gap energy nearly linearly changes with the composition (x) in this range.

Secondly, the temperature dependence of the Hall mobility of InN_xAs_{1-x} is calculated in the temperature range of 30–600 K for $x = 0.0$ and $x = 0.01$, which is shown in figure 2. The carrier concentration of InAs is taken as 10^{16} cm^{-3}. Figure 2 shows the effects of temperature on the Hall mobility for InAs and $InN_{0.01}As_{0.99}$. The Hall mobility of InAs reaches the maximum value of 83,054 cm^2/Vs at 60 K. The Hall mobility of InAs is 76051 cm^2/Vs at 77 K and 12546 cm^2/Vs at 300 K. The Hall mobility of $InN_{0.01}As_{0.99}$ alloy is about 18,000 cm^2/Vs at 77 K, and about 6000 cm^2/Vs at 300 K. The last value
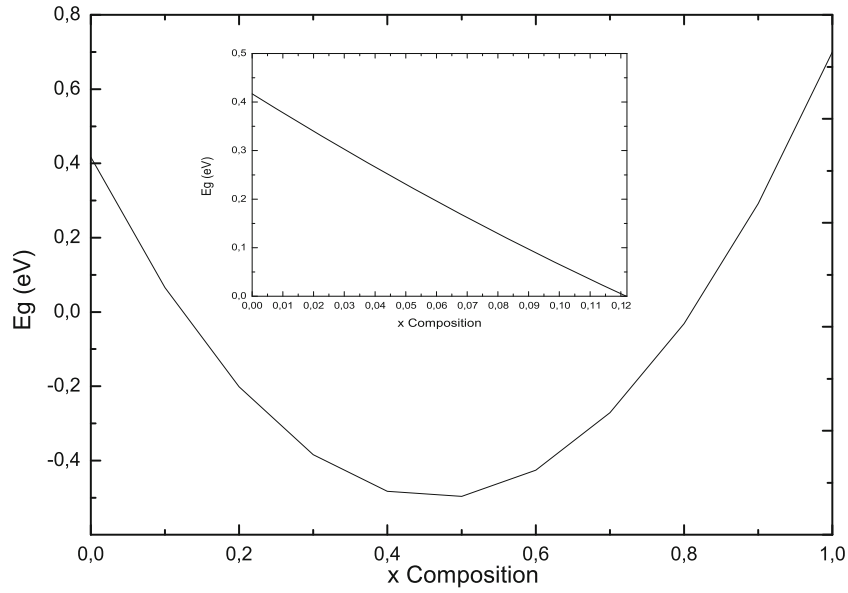
Figure 1. The composition (x) dependence of the energy band gap in InN$_x$As$_{1-x}$. The inset shows the composition dependence of the energy band gap in the range of 0.0 to 0.1218.
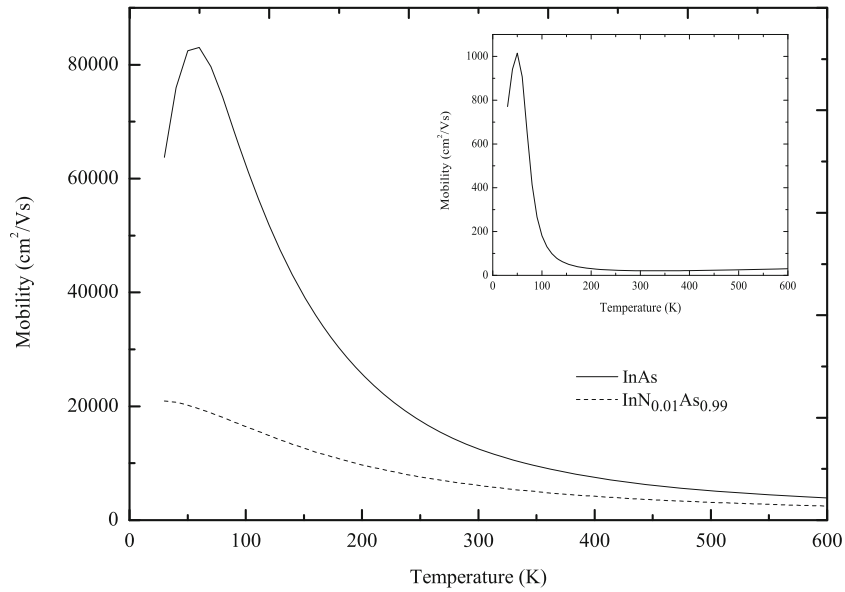
Figure 2. The variation of Hall mobility with temperature for InAs and InN$_{0.01}$As$_{0.99}$. The inset shows the temperature dependence of Hall mobility for InN$_{0.1218}$As$_{0.8782}$.
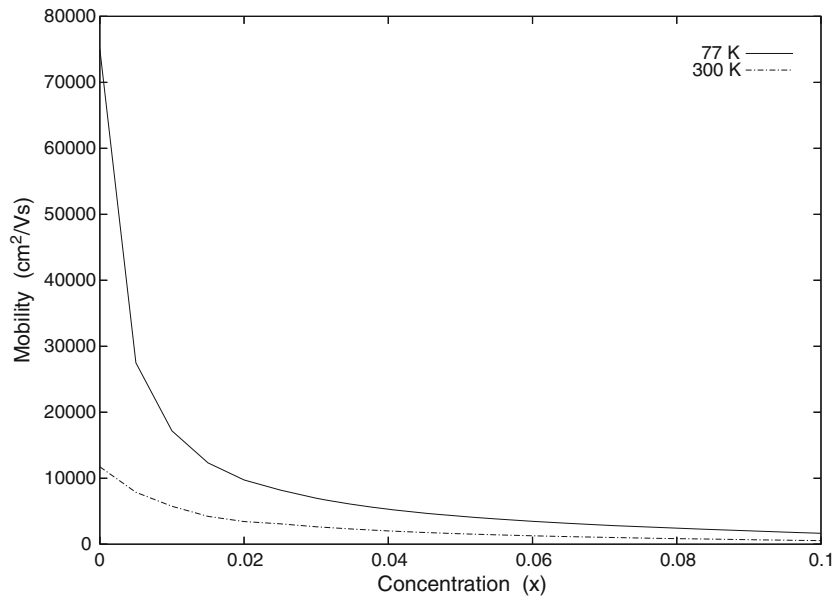
Figure 3. Hall mobility vs. the concentration x at 77 and 300 K for $InAs_{1-x}N_x$.

(about 6000 cm^2/Vs at 300 K) is obtained very close to the value (6000 cm^2/Vs at 293 K) experimentally measured by Zhuang and Krier [25]. The Hall mobility is 11282 cm^2/Vs, 5060 cm^2/Vs, 3098 cm^2/Vs and 477 cm^2/Vs at 77 K, and about 4143 cm^2/Vs, 1846 cm^2/Vs, 981 cm^2/Vs and 21 cm^2/Vs at 300 K when the N content is 0.02, 0.06, 0.1 and 0.1218, respectively. The inset in figure 2 shows that the Hall mobility of InN_xAs_{1-x} changes with the temperature (30–600 K). The Hall mobility of $InN_{0.1218}As_{0.8782}$ alloy reaches a maximum value of 1015 cm^2/Vs at 50 K. It is illustrated in figure 2 that the Hall mobility of InAs fairly decreases with the addition of a small amount of nitrogen. Because of the variation of the energy band gap and the electron effective mass with the low composition of nitrogen in InAs, the conduction band becomes highly non-parabolic, which further affects the Hall mobility. Due to the non-parabolicity of the conduction band, the effective mass of the electrons increases resulting in a sharp reduction in the Hall mobility [9].

In figure 3, it is shown that the Hall mobility of InN_xAs_{1-x} changes with the nitrogen concentration x at 77 and 300 K. The Hall mobility at 77 K quickly decreases up to $x = 0.02$ and rather slowly diminishes above this value. The mobility at 300 K decreases slower than the mobility at 77 K. However, the mobility of InN_xAs_{1-x} at 300 K diminishes similar to its mobility at 77 K if the mole fraction x is above 0.02. It is accepted that a small amount of nitrogen atoms is randomly distributed in InAs compound in alloy formation process. N atoms introduce a strong perturbation to the band structure of InAs. This leads to strong alloy scattering. The Hall mobility decreases by the strong alloy disorder scattering acquired with increasing N composition. This is also reported by others [9,23,34,45,46].

4. Conclusions

In the present study, it is found that the energy band gaps of the InN$_x$As$_{1-x}$ alloys have negative values for the range of $0.1218 < x < 0.8111$. The InN$_x$As$_{1-x}$ alloys behave as metal in this interval [8]. Since the conduction band edge is a mixing state caused by the strong perturbation introduced by smaller nitrogen atoms on arsenic sites, the increase of nitrogen concentration in the InN$_x$As$_{1-x}$ alloys changes the curvature of the conduction band edge around the Γ point. Thus, the corresponding electron effective mass in the InN$_x$As$_{1-x}$ alloys around the Γ point increases with a small value of the N concentration [9]. Because of this, the Hall mobility was considerably decreased by doping InAs with nitrogen at the concentration $x = 0.01$.

It is observed that the ionized impurity scattering at low temperatures (below 60 K) and polar optic phonon scattering at high temperatures (above 100 K) are dominant scattering mechanisms in changing the mobility of InAs with the temperature. The polar optic phonon scattering for InN$_{0.01}$As$_{0.99}$ becomes important above 100 K. Since N atoms randomly distributed in InAs cause a strong perturbation to the band structure of InAs, the alloy disorder scattering is dominant in InN$_x$As$_{1-x}$ alloys. Thus, the alloy scattering increases with the increase in concentration of N from 0.0 to 0.1, but the ionized impurity scattering is not significant.

In conclusion, InN$_x$As$_{1-x}$ has a high mobility for x ranging from 0.0 to 0.1218. The energy band gaps of these alloys have negative values in the range of $0.1218 < x < 0.8111$ and exhibit metallic behaviour. From figure 3, it is seen that the Hall mobility decreases up to $x = 0.02$ and rather slowly diminishes above this value for both temperatures. This study supports the following statements. Even for low concentrations ($x \leq 0.02$), the incorporation of nitrogen causes a strong perturbation of conduction band structure. The mobility of InN$_x$As$_{1-x}$ at $x \leq 0.02$ is affected by the localized electronic states associated with single N impurity as well as N aggregates such as N–N pairs and clusters. That is, N impurities and N–N pairs are localized close to the conduction band edge. This leads to strong scattering centres and less mobility [24,25,47]. Due to these, the InN$_x$As$_{1-x}$ alloys are useful materials for electronics devices and lasers operating in the infrared region.

References

[1] R Bhat, P S Dutta and S Guha, *J. Crystal Growth* **310**, 1910 (2008)
[2] A Y Polyakov *et al*, *J. Appl. Phys.* **73(6)**, 2882 (1993)
[3] V N Brudnyi, N G Kolin and A I Potapov, *Semiconductors* **37(4)**, 390 (2003)
[4] S Kalem *et al*, *Appl. Phys. Lett.* **53(7)**, 562 (1988)
[5] S Dhar and S Ghosh, *J. Appl. Phys.* **86**, 2668 (1999)
[6] D C Look, J R Sizelove *et al*, *Solid State Commun.* **102**, 297 (1997)
[7] C G Van de Walle, M D McClustey *et al*, *Mater. Sci. Eng.* **B59**, 27 (1999)
[8] M Farahmand, C Garetto *et al*, *IEEE Trans. Electron Devices* **48(3)**, 535 (2001)
[9] R Mohammed and S Katrcolu, *J. Alloys Compounds* **469**, 504 (2009)
[10] D R Hang *et al*, *Physica* **E22**, 308 (2004)
[11] M Kuroda, A Nishikawa, R Katayama and K Onabe, *J. Crystal Growth* **278**, 254 (2005)
[12] H Naoi, Y Naoi and S Sakai, *Solid State Electron.* **41(2)**, 319 (1997)
[13] I Vurgaftman, J R Meyer and L R Rom-Mohan, *J. Appl. Phys.* **89(11)**, 5815 (2001)

[14] H Naoi, D M Shaw, Y Naoi, G J Collins and S Sakai, *J. Crystal Growth* **222**, 511 (2001)
[15] H Benaissa, A Zaui and M Ferhat, *J. Appl. Phys.* **102**, 113712 (2007)
[16] S Fahy, A Lindsay and E P O'Reilly, *IEE Proc.-Optoelectron.* **151(5)**, 352 (2004)
[17] T D Veal, L F J Piper, P H Jefferson, I Mahboob, C F McConville, M Merrick, T J C Hosea, B N Murdin and M Hopkinson, *Appl. Phys. Lett.* **87**, 182114 (2005)
[18] Y-T Lin, T-C Ma, T-Y Chen and H-H Lin, *Appl. Phys. Lett.* **93**, 171914 (2008)
[19] R Kudrawiec, *J. Appl. Phys.* **105**, 063529 (2009)
[20] N Tit and M W C Dharmawardana, *Appl. Phys. Lett.* **76(24)**, 3576 (2000)
[21] L Zoppi, M Peressi and M Tosolini, *IEE Proc.-Optoelectron.* **151(5)**, 263 (2004)
[22] L A Pozhar, *The Eur. Phys. J.* **D57**, 343 (2010)
[23] T D Das, A Mondal and S Dhar, *IEE International Workshop on the Physics of Semiconductor Devices (IWPSD)*, 511 (2007)
[24] A Patane, G Allison, L Eaves, N V Kozlova, Q D Zhuang, A Krier, M Hopkinson and G Hill, *Appl. Phys. Lett.* **93**, 252106 (2008)
[25] Q Zhuang and A Krier, *IET Optoelectron.* **3(6)**, 248 (2009)
[26] S Kuboya, M Kuroda, R Katayama and K Onabe, *J. Crystal Growth*, **323(1)**, 26 (2011)
[27] D L Rode, Low-field electron transport, In: R K Willardson, A C Beer (Eds.), *Semiconductors and Semimetals* (Academic Press, New York, London, 1975) Vol. 10
[28] D L Rode, *Phys. Rev.* **B2**, 1012 (1970)
[29] B R Nag, *Electron transport in compound semiconductors* (Springer-Verlag, Berlin, 1980)
[30] B R Nag and G M Dutta, *Phys. Status Solidi* **71**, 401 (1975)
[31] S Li Sheng, *Semiconductor physical electronic* (Plenum Press, New York, 1993)
[32] B K Ridley, *Quantum processes in semiconductors* (Clarendon Press, Oxford, New York, 1982)
[33] D C Look, J R Sizelove, C E Stutz, K R Evans and D W Whitson, *J. Appl. Phys.* **71(1)**, 260 (1992)
[34] W Li, M Pessa and J Likonen, *Appl. Phys. Lett.* **78(19)**, 2864 (2001)
[35] V W L Chin, *J. Phys. Chem. Solids* **52(9)**, 1193 (1991)
[36] V W L Chin, T L Tansley and T Osotchan, *J. Appl. Phys.* **75**, 7365 (1994)
[37] D C Look, H Lu *et al*, *Appl. Phys. Lett.* **80(2)**, 258 (2002)
[38] E S Hwang, E M Park *et al*, *J. Korean Phys. Soc.* **48(1)**, 93 (2006)
[39] A F M Anwar, S Wu and R T Webster, *IEEE Trans. Electron Devices* **48(3)**, 567 (2001)
[40] H Morkoc, *Nitride semiconductors and devices* (Springer-Verlag, Berlin, Heildelberg, New York, 1999)
[41] C G Rodridgues, V N Freire, A R Vasconcellos and R Luzzi, *Mater. Res.* **6**, 1 (2003)
[42] S Aydogu and O Ozbas, *Mater. Sci. Semiconductor Processing* **8**, 536 (2005)
[43] G Satyanadh, R P Joshi, N Abedin and U Singh, *J. Appl. Phys.* **91(3)**, 1331 (2002)
[44] S Strite and H Morkoc, *J. Vac. Sci. Technol.* **1B(10)**, 1237 (1992)
[45] S Fahy and E P O'Reilly, *Appl. Phys. Lett.* **83(18)**, 3731 (2003)
[46] S Fahy and E P O'Reilly, *Physica* **E21**, 881 (2004)
[47] N Miyashita, Y Shimizu and Y Okada, *J. Appl. Phys.* **102**, 044904 (2007)